EFFECT OF DEFECTS ON THERMAL TRANSPORT PROPERTIES OF CNR-GRAPHENE SHEETS

Gang SHI, Changping YIN, Jianwei ZHANG, Su JU and Dazhi JIANG*

Department of Materials Science and Engineering, National University of Defense Technology, Changsha, Hunan 410073, People's Republic of China
Email: shigang4056920@126.com
Email: ychangping@nudt.edu.cn
Email:jwzhang.nudt@gmail.com
Email: suju-nudt@nudt.edu.cn
Email: jiangdz@nudt.edu.cn

Keywords: CNR-Graphene nanostructure, defects, thermal conductivity, molecular dynamics

Abstract
Recently, the 3D nanostructures of graphene sheets and carbon nanorings have received more attention in both experimental and theoretical studies. The existence of defects in the CNR-graphene junctions which usually occurred can affect thermal conductivity of the nanostructure sheets. In the paper, the molecular dynamic simulation method is used to investigate how defects in the CNR-graphene junctions affect thermal transport properties of the CNR/Graphene nanostructure. The CNR/graphene nanostructure is constructed by combining graphene sheets and (6,6) CNRs. The atom vacancy CNR joints, sp^2/sp^3 hybrid covalent bonding CNR joints, and van der Waals interaction CNR joints are investigated here. Results show that the thermal resistance of an atom vacancy CNR-graphene junction is much more dependence with concentration of the vacancies, junctions with sp^2/sp^3 bonds are found to have an inefficient thermal transport property, and van der Waals interaction is an impossible way to overcome the limiting thermal conduction. Analysis based on the vibrational density of states medium theory (VDOS) indicates that sensitivity of the defect concentration originates from the scattering of phonons by defects.

1. Introduction

Carbon nanotubes (CNTs) and single layer graphene, have been demonstrated to show superior thermal, electrical, and mechanical properties attractive for a wide range of potential applications.[1, 2] However, CNTs and graphene exhibit strong direction-dependent thermal and electrical transport properties with extremely low out-of-plane conductivities.[3] A special 3D CNTs/graphene composites, pillared graphene structures (PGS) with CNT as pillars and single layer graphene as floors have attracted much attention. PGS, parallel graphene layers supported by vertically aligned carbon nanotubes, possess desirable transport and mechanical properties while maintaining the excellent properties of their building blocks. Dimitrakakis first designed CNT-graphene 3D nanostructures, and found its capable of enhancing hydrogen storage.[4] Theoretical studies showed that this 3D pillared CNT graphene structure can be used for hydrogen storage[5], efficient electrodes for fuel cells[6], light-weight foamlike, structural materials,[7] tunable multi-dimensional thermal interface materials and thermal rectifiers.[8]

The PGS structure has previously been proposed to address anisotropic thermal properties, and direct molecular dynamics simulations have been used to predict the associated thermal conductivity. Varshney et al.[9] first investigated the thermal transport in pillared-graphene, and concluded that the length of pillars and the inter-pillar distance are the two parameters governing its thermal transport. In addition, Shi et al. [10] built a network model with the junction resistance R_j to estimate the effective thermal conductivity, and the results agree well with direct MD simulation data. From their work, they concluded that thermal resistance of pillared graphene structure is dominated by the CNT-graphene junction resistance. So junctions are the key component for 3D CNT-graphene hybrid nanostructures attractive for numerous innovative applications. Jianbing Niu et al. simulated the growth of a carbon

Excerpt from ISBN 978-3-00-053387-7

nanotube on a graphene sheet with Fe nanoparticles as catalyst by quantum mechanical molecular dynamics (QM/MD) methods, found that the junctions with covalent C-C bonds could be formed during the CNT growth on graphene.[11] Yu Zhu et al. first showed an atomic resolution junction between the two carbon materials and observed the covalent transformation of sp^2 carbon between the planar graphene and the single-walled carbon nanotubes at the atomic resolution level, the result is consistent with the conjugated seven-membered-ring-containing junctions suggested by theoretical studies. [12] Both Jianbing Niu'work and Yu Zhu'work indicate that CNT intercalated growth between graphene layers.

In general, defects inevitably exist in graphene and CNT during the preparation process, such as vacancies, stone-wales of dislocations, impurities and other non-topological structural defects. And new defects formed during the intercalation of CNTs at the interlayer of graphene. In addition connection between the CNTs and graphene was not studied exhaustively. Although studies show that the carbon atoms at the CNT–graphene interface may be sp^2 bonded. Due to the numerous possibilities of attachment between the nanotube and graphene sheet whether there are all covalent bonds that link the graphene and CNTs it could be that many of those CNTs are physical absorption on the graphene plane, or conjoined by sp^3 carbon to sp^3 carbon. While much research has been conducted on the mechanical and thermal transport properties of graphene, there has been less work focused on the effect of defect in CNT-graphene junctions on the thermal conductivity. The effect of defect on the thermal conductivity of 3D nanostructures is not fully understood at present.

CNTs in the architectures above could not act as effective heat transport tunnels to enhance the out-of-plane thermal transport between graphene sheets. These architectures reported still suffered from the through-plane thermal conductivity. our previous research results prove super-short CNTs (namely carbon nano-rings, CNRs) linked graphene.[13] The main goal of this study is to investigate how CNR-graphene junction defect affect the thermal transport characteristics in these hybrid structure. In this regards, we study thermal transport in such junctions with different types defects, sp^2/sp^3 bonding and vacancies. In order to better understand phonon scattering in these structures, the phonon density of states (DOS) are calculated and compared.

2. MOLECULAR DYNAMICS SIMULATION

2.1 Models

All models simulating CNR-graphene nanostructure were built based on Materials Studio (Accelrys Inc). To construct the CNR-graphene junctions, two parallel graphene sheets were built in a periodic boundary condition. Circular holes were created on the graphene sheets and an armchair CNR was placed vertically over the pore with the tube ends bonded to the graphene sheets respectively. The diameter of the pores is the same as that of CNRs. A 30 Å thick vacuum slab along the z-axis direction was built to prevent any interaction between the periodic graphene sheets. Figure 1 (a) shows the top view of a graphene hybrid structure with one CNR. The CNR is oriented along *z*-axis. In all simulated cases, the geometries of the graphene and their overlapping areas were fixed (Figure 1 (b)), that is, the overlap length, ΔL=4.5 nm, length of graphene sheet one, L_1=9 nm, length of graphene sheet two, L_2=16.5 nm, the total length of the hybrid structure, $L=L_1+L_2-2\Delta L$=24.5 nm (along the *x*-axis direction), the width of the graphene sheets (along the *y*-axis direction), W= 4.26 nm. Figure 2 shows the schematic of a CNR-graphene junction. A junction region is consist of two overlapped graphene parts and a CNR joint. Figure 3 shows the schematic of different joints. A perfect sp^2 bonding CNR marked as CNR, the CNR joint bonding by sp^2/sp^3 hybrid bond marked as CNR-sp^2/sp^3, the CNR joint bonding by van de Waals interaction marked as CNR-van. Carbon atom vacancy joint marked as CNR-v*x*, where *x* means the number of vacancies, for example, a carbon atom vacancy joint marked as CNR-v1.

2.2 Computational methods

In this work, reverse non-equilibrium molecular dynamics (RNEMD) is employed to obtain thermal conductivity and thermal resistance in CNR-graphene junction region, using the COMPASS II force field to account for the carbon-carbon interactions. The simulation structure is energy-minimized to reach equilibration by iteratively adjusting atomic coordinates. The unit cell is partitioned into 50 slabs along the x-axis for temperature recording and momentum exchange processes. NEMD method is applied to all models in constant volume and constant energy ensemble (NVE). According to Muller-Plathe algorithm, heat sink and source were placed at the center and each end of the cells to generate

Excerpt from ISBN 978-3-00-053387-7

constant heat flux, as showed in Figure 1 (a). When the simulation systems reached steady state after 125 ps, the production stage were put to run for another 250 ps[16-17]. The final interfacial thermal resistance value was calculated by averaging the data collected over the 250 ps period in the steady state.
The transferred heat is calculated as the accumulation of exchanged kinetic energy as:

$$Q = \sum_{\text{swaps}} \left(E_h - E_c \right) \tag{1}$$

where E_c and E_h are kinetic energy of the cold and hot slabs, respectively. The heat flux J through the structure was imposed following the NEMD simulation method. When the heat flow in the structure reached a steady state, the heat flux and temperature gradient was recorded and averaged. The imposed heat flux J is calculated from:

$$J = \frac{Q}{2A\Delta t} \tag{2}$$

where A is the area normal to the direction of heat flux and Δt is the simulation time. The thickness of both graphene and CNR walls are assumed to be 1.42 Å, which is the generally accepted C-C bond length and has been used in literatures to obtain thermal conductivity of graphene or CNTs[14].
In addition, the interfacial thermal resistance, R, can be calculated from the temperature jump in the temperature profile across the thermal interface using:

$$R = \frac{\Delta T}{J} \tag{3}$$

In order to understand the mechanism of thermal conduction, phonon spectrum of atoms on the sides of the model is calculated. The phonon spectrum function $P(\omega)$ can be obtained by Fourier transform of the velocity autocorrelation function which can be expressed as follows:

$$P(\omega) = \frac{1}{\sqrt{2\pi}} \int e^{-i\omega t} \left(\sum_{j}^{N} v_j(t) v_j(0) \right) dt \tag{4}$$

where ω is vibrational wavenumber of the phonon, $v_j(t)$ is velocity of atom j at time t, N is atomic number and $v_j(0)$ is velocity of atom j at initial time.
To probe the underlying mechanisms of the effect of cross-linker on graphene interfacial thermal resistance, the VDOS for pristine graphene and CNR joint were calculated.
To quantitatively determine the overlap of two VDOS spectra, an overlap factor is defined as[10]:

$$\eta = \int_0^{+\infty} \min\left[P_1(\omega), P_2(\omega) \right] d\omega \tag{5}$$

P_1 and P_2 are the normalized VDOS of region 1 and region 2. The numerator of η means the overlap area between region 1 and region 2. The denominator of η means the normalized VDOS area of a region. A small overlap factor η indicates a poor overlap between the two spectra possess, a big overlap factor η means a small mismatch between two regions.

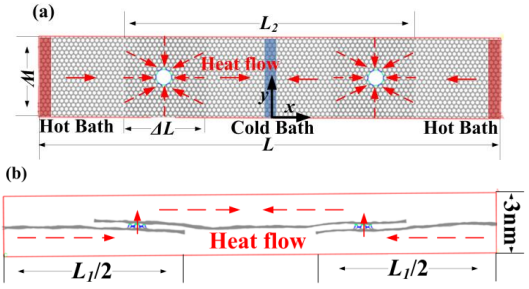

Figure 1. Schematic of a CNR-graphene nanostructure

Excerpt from ISBN 978-3-00-053387-7

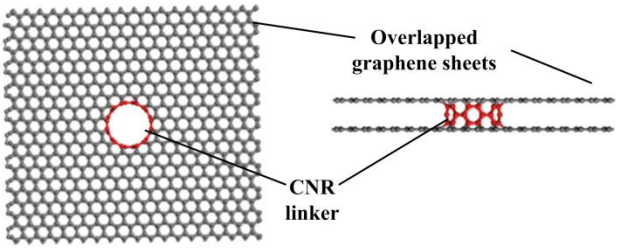

Figure 2. Schematic of a CNR-graphene junction

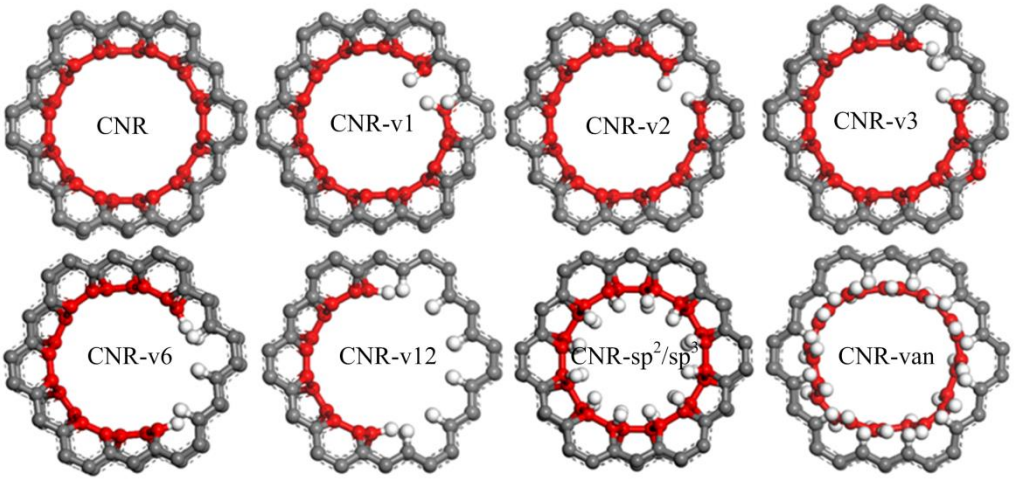

Figure 3. Schematic of CNR joints

3. Result and discussion

First of all, in order to validate the models used herein, thermal conductivity of a monolayer graphene sheet with a length of 24.5 nm and a width of 2.46 nm was calculated. By assuming the thickness of the graphene sheet as 1.42 Å, thermal conductivity of the monolayer graphene sheet was calculated to be 247.5±17.7 W/mK. (thermal conductivity, $\lambda = J/(2A\partial T/\partial x)$, where $\partial T/\partial x$ is the temperature gradient). The result was in good agreement with the reported value of ~230 W/mK for a 25 nm long graphene sheet in Lanqing Xu's work[14]. In order to validate junction resistance, a overlapped graphene sheet thermal resistance was calculated, the result is 1.47±0.06 Km^2/GW.

3.1 Vacancies Concentration Dependence

Figure 4 shows the variation of the temperature across CNR-graphene nanostructure. The temperature profile for a perfect sp^2 covalent junction is also calculated for contrast, shown in Figure 4(a). For all models exhibit a much high temperature gradient at junction positions. Owing to the presence of the CNR-Graphene junction, there exists a temperature jump, ΔT, at the junction region. Furthermore, the larger the number of vacancy defects, the bigger the temperature jumps, which is shown in Figure 4 (b)~(f).

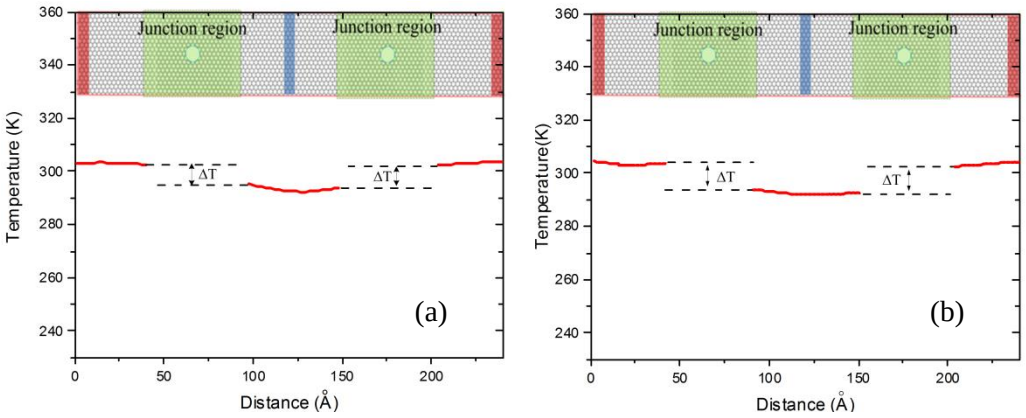

Excerpt from ISBN 978-3-00-053387-7

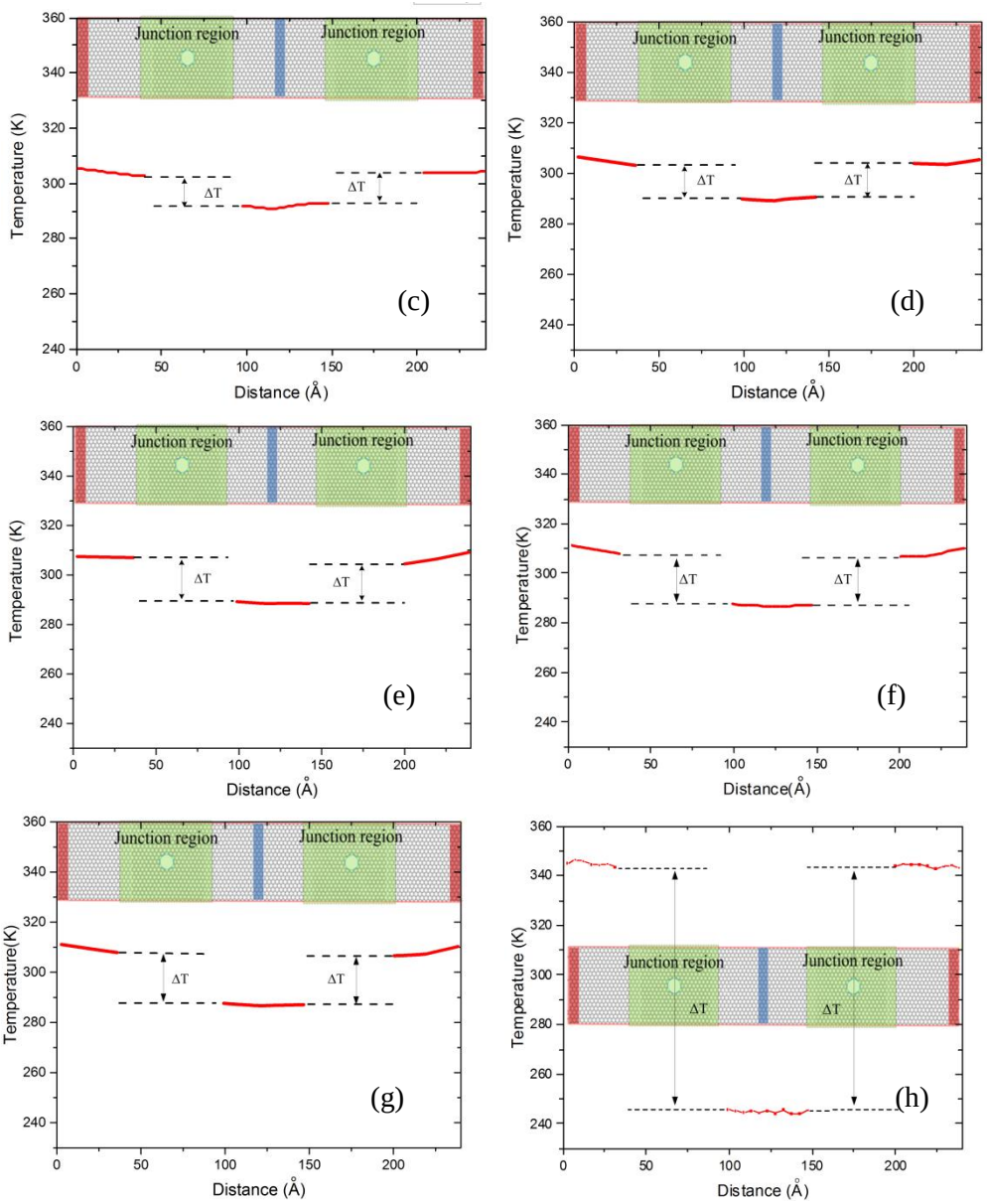

Figure 4. Temperature profiles along CNR-graphene nanostructure with: (a) a perfect sp^2 covalent junction, (b) a carbon atom vacany, (c) two carbon atom vacancy junction, (d) three carbon atom vacancy junction, (e) six carbon atom vacancy junction, (f) twelve carbon atom vacancy junction, (g) a sp^3 covalent junction, (h) a van de wall junction

Based on eq 3, the junction thermal resistance R can be obtained by MD simulations for different defective CNR-graphene nanostructure. Figure 5 displays the junction thermal resistance with vacancy defects. For a junction with perfect sp^2 covalent bonding CNR, the thermal resistance is 0.135 ±0.002 Km^2/GW. When defect concentration is low, junction thermal resistance increased slightly. When vacancies is half of total atoms on CNR, thermal resistance increased to 0.25±0.02 Km^2/GW, near twice of perfect CNR-graphene junction.

A small number of vacancy defects cause a little thermal resistance increment and more defects cause a larger junction thermal resistance. This phenomenon can be explained by phonon scattering. For a perfect CNR Joint, the phonon scattering is due solely to inharmonic vibrations of atoms, while, for CNR-graphene with topological defects, the phonon scattering may be induced by defects as well as by inharmonic vibrations. At a low defect concentration, the defects serve as local scattering centers. While at high concentrations, different scattering centers interact with each other.

To gain a better understanding of the junction thermal resistance, the VDOS of different joints and graphene were calculated, as shown in Figure 6. As shown in table 1, the overlap factor η for

Excerpt from ISBN 978-3-00-053387-7

decreased as vacancies increases. In our results, it is found that the VDOS of the CNR is sensitive to vacancy concentration. Previous research[15]also indicated that the thermal conductivity of CNTs or graphene decreases significantly with increasing defect concentrations.

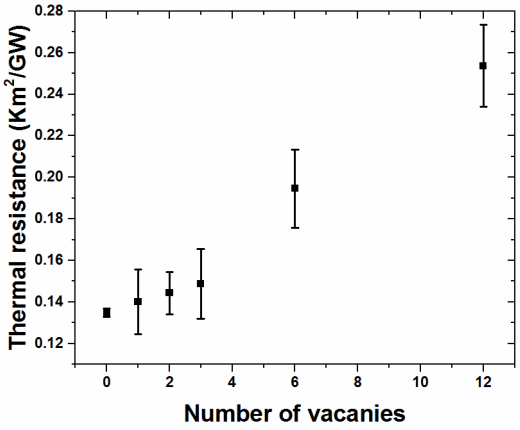

Figure 5. Junction thermal resistance with respect to the number of vacancies

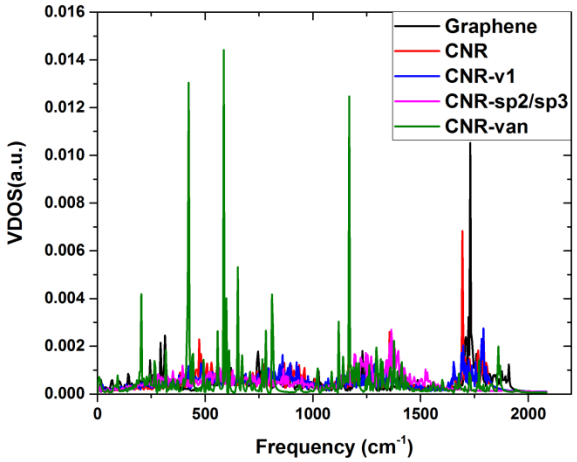

Figure 6. VDOS of graphene and different CNR jonits

Table 1. LDOS overlap factor for different CNR

Joint	CNR	CNR-V1	CNR-V2	CNR-V3	CNR-V6	CNR-V12	CNR-sp^2/sp^3
η	0.690	0.684	0.680	0.679	0.665	0.647	0.606

3.2 sp^2/sp^3 junction

Figure 4 g shows a typical temperature profile of the middle CNT pillar and two graphene sheets with sp^2 covalent junctions. An temperature jump exists at the junction, while the temperature distributions are nearly linear.

With regards to a sp^2 covalent bonding CNR-graphene junction, junctions with mixed sp^2/sp^3 bonds are observed to have a much higher thermal resistance. The calculated thermal resistance is about 0.23±0.01 Km^2/GW. It is known that sp^3 hybridized C-C bonds in carbon nanotubes or graphene play the role of a structural defect during thermal transport. Figure 6 shows the VDOS of sp^2/sp^3 bonds CNR. It can be seen that the VDOS overlapping area is small and η is 0.606. Junctions with sp^2/sp^3 bonds are found to have an inefficient thermal transport property.

3.3 van der Waals junctions

Figure 4 h displays the typical temperature gradients of CNR-graphene nanostructure with van der Waals junction. The calculated R is 1.46±0.02 Km^2/GW, which is almost as same as the interface thermal resistance of overlapped graphene sheets. It is the result of weak bonding of van der Waals

Excerpt from ISBN 978-3-00-053387-7

interaction. This is consistent with previous experimental observations of bonding effects on thermal interfacial transport. For van der Waals junctions, the atoms near the boundary have very weak interactions with atoms on the other side of the junction, and therefore, their local DOS is little modified, in contrast to the sp^2 covalent junction. So a van der Waals joint could not help to overcome the limiting thermal conduction between graphene sheets .

4. Conclusions

In summary, the thermal transport across CNR−graphene junctions has been investigated via MD simulations. Based on the simulation results, it is found that sp^2 covalent bonding significantly promoted the thermal transport across CNR-graphene interfaces. The absence of carbon atoms leads to an increment of interfacial thermal resistance, and this increment is linearly dependent on the vacancy number at a low defect concentration. Junctions with sp^2/sp^3 bonds are found to be an inefficient way to improve thermal transport property of CNR/graphene nanostructure. While, Van der Waals junction did not decrease the thermal resistance between overlapped sheets distinctly because of weak bonding. Our simulation results provide useful guidelines on the selection of appropriate joints for enhancing CNR-graphene interfacial thermal transport. The findings herein should be useful for the future development of super thermal conductivity carbon nano-phased materials.

Acknowledgments

This work was supported by Natural Science Foundation of China (No.11202231).

References

[1] J. Che, T. Cagin and W.A. Goddard III. Thermal conductivity of carbon nanotubes, *Nanotechnology*, 11:65-69, 2000.
[2] A.A. Balandin. Thermal properties of graphene and nanostructured carbon materials, *Nature Materials*, 10:569-581, 2011.
[3] E. Pop, V. Varshney and A.K. Roy. Thermal properties of graphene: Fundamentals and applications, *MRS Bulletin*, 37:1-21, 2012.
[4] G.K. Dimitrakakis, E. Tylianakis and G.E. Froudakis. Pillared Graphene: A New 3-D Network Nanostructure for Enhanced Hydrogen Storage, *Nano Letters*, 8: 3166-3170, 2008.
[5] Investigation on the existence of optimum interlayer distance for H2 uptake using pillared-graphene oxide, *international journal of hydrogen energy*, 37:14217-14222, 2012,
[6] Z. Fan, J. Yan, L. Zhi, Q. Zhang, T. Wei, J. Feng, M. Zhang, W. Qian and F. Wei. A Three-Dimensional Carbon Nanotube/Graphene Sandwich and Its Application as Electrode in Supercapacitors, *Advanced Materials*, 22:3723-3278, 2010.
[7] C.-H. Wang, T.-H. Fang and W.-L. Sun. Mechanical properties of pillared-graphene nanostructures using molecular dynamics simulations, *Journal of Physics D: Applied Physics*, 47:1-8, 2014.
[8] W. Feng, M. Qin, P. Lv, J. Li and Y. Feng. A three-dimensional nanostructure of graphite intercalated by carbon nanotubes with high cross-plane thermal conductivity and bending strength, *Carbon*, 77:1054-1064, 2014.
[9] V. Varshney, S.S. Patnaik, A.K. Roy, G. Froudakis and B.L. Farmer. Modeling of Thermal Transport in Pillared-Graphene Architectures, *American Chemical Society*, 4:1153–1161, 2010.
[10] J. Shi, Y. Dong, T. Fisher and X. Ruan. Thermal transport across carbon nanotube-graphene covalent and van der Waals junctions, *Journal of Applied Physics*, 118:044302-044307, 2015.
[11] J. Niu, M. Li, W. Choi, L.D. c and Z. Xia. Growth of junctions in 3D carbon nanotube-graphene nanostructures: A quantum mechanical molecular dynamic study, *Carbon*, 67:627-634, 2014.
[12] Y. Zhu, L. Li, C. Zhang, G. Casillas, Z. Sun, Z. Yan, G. Ruan, Z. Peng, A. Raji, C. Kittrell, R.H. Hauge and J. Tour. A seamless three-dimensional carbon nanotube graphene hybrid material, *Nature Communications*, 3:1225, 2012.
[13] J. Zhang, G. Shi, C. Jiang, S. Ju and D. Jiang. 3D Bridged Carbon Nanoring/Graphene Hybrid Paper as a High-Performance Lateral Heat Spreader, *small*, 46:6197-6204, 2015.
[14] L. Xu, N. Wei, Y. Zheng, Z. Fan, H.-Q. Wang and J.-C. Zheng. Graphene-nanotube 3D networks: intriguing thermal and mechanical properties, *Journal of Materials Chemistry A*, 22:1435-1444, 2012.

Excerpt from ISBN 978-3-00-053387-7

[15] F. Hao, D. Fang and Z. Xu. Mechanical and thermal transportation properties of graphene with defects *Applied Physics Letters*, 99:041901-041903, 2011.

Excerpt from ISBN 978-3-00-053387-7